GEM-based detectors for SR imaging and particle tracking

2012 JINST 7 C03021

(http://iopscience.iop.org/1748-0221/7/03/C03021)

PUBLISHED BY IOP PUBLISHING FOR SISSA MEDIALAB

RECEIVED: *January 12, 2012*
ACCEPTED: *February 20, 2012*
PUBLISHED: *March 12, 2012*

2nd INTERNATIONAL CONFERENCE ON MICRO PATTERN GASEOUS DETECTORS,
29 AUGUST – 1 SEPTEMBER 2011,
KOBE, JAPAN

GEM-based detectors for SR imaging and particle tracking

L.I. Shekhtman,,[a,b,1] V.M. Aulchenko,[a,b] A.E. Bondar,[a,b] A.D. Dolgov,[b] V.N. Kudryavtsev,[a] D.M. Nikolenko,[a] P.A. Papushev,[a] E.R. Pruuel,[c] I.A. Rachek,[a] K.A. Ten,[c] V.M. Titov,[a] B.P. Tolochko,[d] V.N. Zhilich[a] and V.V. Zhulanov[a,b]

[a] *Budker Institute of Nuclear Physics SB RAS,*
11 Lavrentiev Avenue, Novosibirsk 630090, Russia
[b] *Novosibirsk State University,*
2 Pirogova str., Novosibirsk 630090, Russia
[c] *Lavrentiev Institute of Hydrodynamics SB RAS,*
Novosibirsk 630090, Russia
[d] *Institute of Solid State Chemistry and Mechanochemistry SB RAS,*
Novosibirsk 630090, Russia

E-mail: L.I.Shekhtman@inp.nsk.su

ABSTRACT: Status of several projects under development in Budker INP with GEM-based detectors for synchrotron radiation imaging and particle tracking is reviewed. These are namely: the detector for imaging of explosions(DIMEX) at SR beam, the detector for WAXS studies at SR beam (OD4), the triple-GEM detectors for the tagging system of KEDR experiment at VEPP-4M collider and the triple-GEM detectors for the tagging system of Deuteron experiment at VEPP-3 storage ring.

KEYWORDS: Electron multipliers (gas); Particle tracking detectors; X-ray diffraction detectors

[1] Corresponding author

doi:10.1088/1748-0221/7/03/C03021

Contents

2012 JINST 7 C03021

1 Introduction

Gas Electron Multiplier (GEM) [1] combines high granularity of the amplifying elements (holes) with very attractive mechanical properties. Cascaded GEM detectors can provide high spatial resolution together with high rate capability. Combination of these features is often necessary in X-ray detectors for the experiments with synchrotron radiation (SR) as well as for the applications in particle physics when tracking detectors are located close to the beam. In the present review the status of several projects that are under development in the Budker Institute of Nuclear Physics, Novosibirsk with single or cascaded GEM detectors are described. All projects are aimed at developing devices or systems that combine high spatial resolution with high rate capability.

The detector for imaging of explosions (DIMEX) is developed for imaging of synchrotron radiation from separate bunches in the storage ring and thus allows viewing an evolution of very fast processes. GEM serves as a screening mesh (Frisch-grid) with adjustable transparency in this detector. Last results with reduced GEM transparency will be demonstrated that allowed improvement of dynamic range of the detector by a factor of 2.

The OD-4 is arc-shaped detector with 350 mm focus distance based on GEM cascade. Readout PCB has 2048 30 mm long radial strips at a pitch of 0.2 mm at the inner side. The detector is planed for operation in counting mode with single discriminator threshold. The first full-size prototype partly equipped with electronics demonstrated good spatial resolution of 0.5 mm (FWHM) as well as high rate capability of 150 kHz/channel with 8 keV photons and Ar-25%CO2 gas mixture at 1 atm.After these measurements the detector concept was significantly reconsidered and new electronics is now being developed.

The tagging system of KEDR detector is a two-shoulder magnetic spectrometer that was designed to measure precisely the momenta of electron and positron that lost their energy through two-photon interaction. 8 triple-GEM detectors with small-angle stereo readout are operating in this system. The first experience after operation during the season 2010-2011 will be reported.

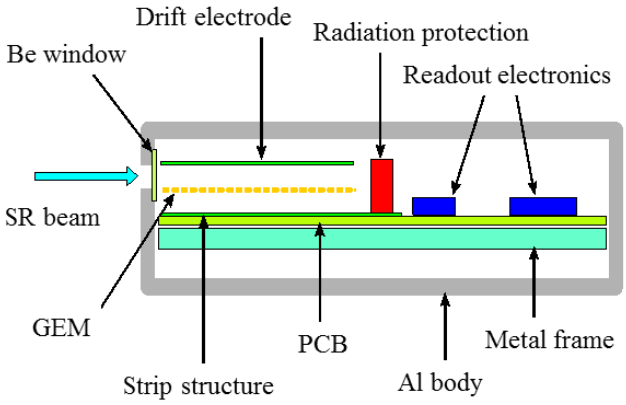

Figure 1. Schematic view of the DIMEX.

The tagging system of Deuteron experiment is a new project that started last year. This will be also a magnetic spectrometer that will measure precisely the momentum of electrons or positrons in the range of 0.1-1 GeV. The detectors should contain as low amount of material as possible in order to reduce multiple scattering.

2 The detector for imaging of explosions at synchrotron radiation beam

The DIMEX is developed for the studies of fast proceses at synchrotron radiation beam by viewing the time evolution of X-ray projection image of an exploding sample or the small angle scattering pattern (SAXS) of an exploding sample [2–5]. The DIMEX allows collection of the signal from individual electron bunch in a SR source without mixing it with the signal from neighbouring bunches. Thus the time resolution of the method is determined by the bunch length but not the time resolution of the detector. In the VEPP-3 storage ring that is used presently for the experiments with the DIMEX the bunch length is about 30 cm and the time gap between bunches is equal to 250 ns in single-bunch mode.

The DIMEX is a high-pressure ionization chamber with multi-strip readout structure (figure 1). Collimated SR beam enters the gas volume filled with mixture of Xe-CO_2 (75-25%) through beryllium window. X-ray photons with average energy $\sim$20 keV are absorbed in the gap between the high voltage drift electrode and the GEM. Primary electrons drift through the GEM that shields multi-strip readout structure from positive ions. The GEM does not amplify primary electrons, but absorbs part of ionization and thus operates as attenuator. Each strip of the readout structure is connected to an input of the integrator chip APC128 [6]. Each of 128 channels of this chip contains a low noise integrator and 32-cells analogue pipe-line that can be read out through an analogue multiplexer.

Complete description of the DIMEX performance was presented elsewhere (see [4, 5]). The detector demonstrates spatial resolution of $\sim$0.2 mm (FWHM), maximal signal-to-noise ratio of $\sim$100 and time resolution better than 50 ns. Maximal frame rate is 8 MHz, frame size is 512 channels and one experiment contains 32 frames. In the present review we describe the last results of the optimization of the detector parameters.

2012 JINST 7 C03021

One of the critical parameters of the DIMEX is maximal photon flux that can be measured. This value determines the best precision of signal measurement that can be achieved. DIMEX is integrating detector and maximum value of the signal is determined by the saturation limit of APC128 integrators. In order to increase the maximal photon flux that can be measured, the signal from one photon has to be reduced. The signal from individual photon can be modified by the help of the GEM. According to general dependances established in [7] the resistive divider that supplies high voltages to the detector electrodes was modified to reduce the GEM transparency. The drift field was increased, while the induction field and the field in GEM holes were reduced. In the optimal fields configuration the drift field was about twice higher than in the initial configuration, the field in the GEM holes and the induction field were twice lower than in the initial configuration. The relative trasparency, that was measured as the ratio of signal with the optimized divider and with the initial divider at fixed conditions of irradiation, was reduced by a factor of 5 in the optimized case.

As a criterion for comparison of the performance with optimized electric fields we chose the registered photon flux, calculated assuming that the image noise is related only to quantum noise. This value is called in literature "noise equivalent quanta" or NEQ [8]. For the comparison of optimized performance with the initial one, the two detectors were used. They are called below as DIMEX1 and DIMEX3. The DIMEX1 detector is the first version of the DIMEX that was used by the users for a long time and comparison of its performance with the new detector is quite important.The DIMEX1 has the resistive divider inside gas volume and thus it can not be changed. The DIMEX3 is the last version of the detector that has the resistive divider outside the gas volume and thus allows for its modification. All main parameters of these versions of the DIMEX are similar except of some design features. NEQ as a function of signal in two different detectors and in one detector with two different resistive dividers is shown in figure 2. In the case of reduced GEM transparency the DIMEX3 detector allows for $\sim$3 times higher registered photon flux at the same value of signal. Thus similar increase in maximal registered photon flux can be expected. DIMEX1 and DIMEX3 are similar, and DIMEX1 had the initial resistive divider. However the drift and the induction gaps in the DIMEX1 could be slightly different from the DIMEX3 that can explain the difference in performance with the same resistive divider.

In figure 3 the results of the measurements of spatial resolution are presented for the detector with reduced GEM transparency. The measurements were performed with the beam positioned below the GEM into the induction gap and above the GEM (normal case). This test was performed because of the suspicion that reduced transparency might cause degradation of the resolution. The results demonstrate that the spatial resolution is preserved within statistical accuracy.

DIMEX with improved dynamic range was successfuly used in the experiments during the season 2010-2011. As an example figure 4 demonstrates the density distribution obtained after processing of the result of the experiment where a cylindrical exploding sample was positioned perpendicular to the SR beam ([9]). In this experiment the cylindrical charge of TATB explosive was fastened such that its axis was perpendicular to the narrow flat beam of SR. The diameter of the charge was 2 cm, the length was about 7 cm, the height of the SR beam was 0.5 mm and the width of the SR beam was close to 2 cm. The detonator was attached to the charge at one end of the cylinder. After the initiation of the detonator, the detonation wave runs along the cylindrical charge. At the same time the DIMEX stores one dimentional images of the SR beam passing

2012 JINST 7 C03021

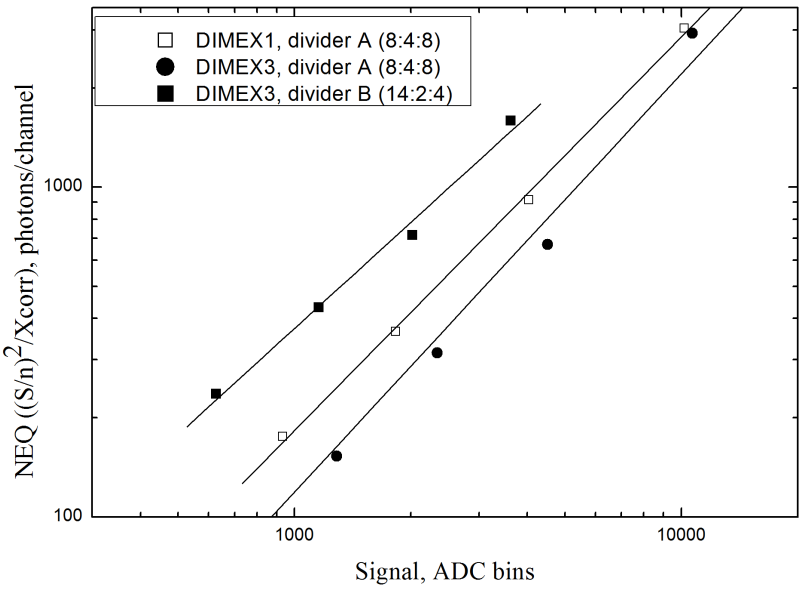

Figure 2. Noise equivalent quanta for different resistive dividers in the DIMEX3 and for initial resistive divider in DIMEX1. The initial divider is called divider A, the optimized divider is called divider B. The numbers in brackets mean the value of resistors in MΩ

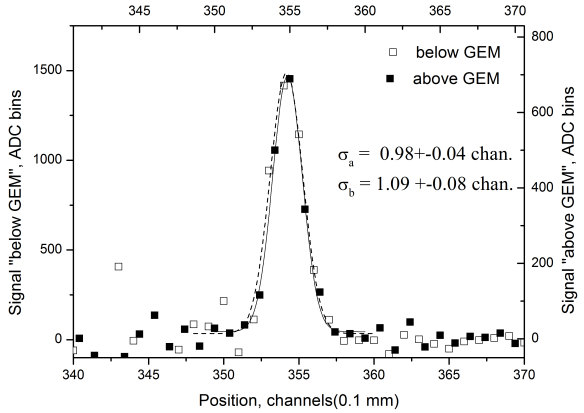

Figure 3. Spatial resolution of the DIMEX (line spread function). Horizontal scale is in channels. Each channel is equal to 0.1 mm. Comparison of irradiation above GEM and below GEM.

through the exploding sample every 500 ns synchronously with the bunches in the storage ring. When the detonation wave reaches the layer where the SR beam passes the sample, the material of the sample at the layer becomes denser and the beam intensity registered by the DIMEX drops. After the detonation wave the sample starts to decay and the beam intensity after the sample starts to grow. As the velocity of the detonation wave is constant, one can recalculate the time after passage of the wave into the distance from the detonation wave. This distance corresponds to the horizontal axis of the plots in figure 4. Assuming that the sample is symmetrical we can recalculate the beam intensity measured by the DIMEX into density of the material as a function of radius in

2012 JINST 7 C03021

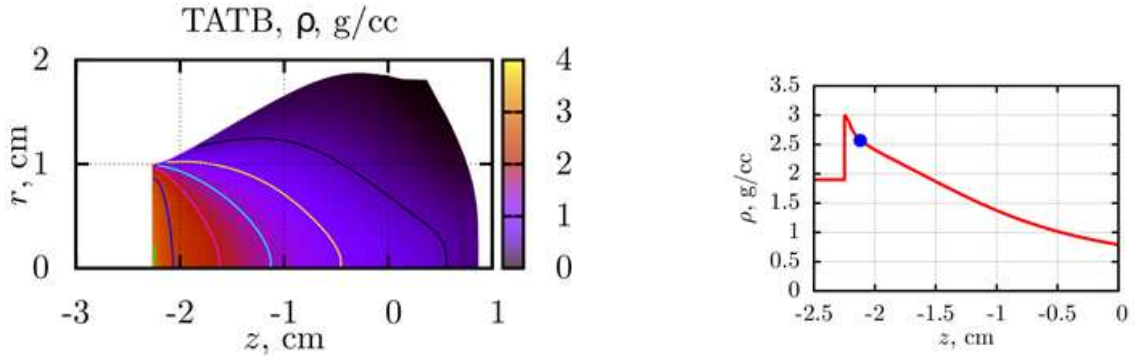

Figure 4. The distribution of density (left) and the value of density along the axis (right) in an exploding cylindrical sample of TATB explosive with initial density of 1.85 g/cc. The image is obtained with the DIMEX with improved dynamic range.

the sample. This density map is shown at the left plot of figure 4. The detonation wave is at Z=-2.5 cm and to the right from the detonation wave the density gradually drops. Particular shape of this density map helps to understand the basic laws of material behavior in the conditions of very high densities and temperatures.

3 OD-4, the detector for WAXS

The detector for wide angle X-ray scattering (WAXS) studies OD4, based on GEM cascade is under development in the Budker INP [10–12]. The OD4 has arc-shaped GEM cascade read out with multi-strip structure with the strips directed to the scattering source. Schematic view of the OD4 is shown in figure 5.

X-rays from the scattering source get into the detector box through beryllium window and are absorbed in the gap between the drift electrode and the top GEM. Primary electrons drift towards the GEM cascade, amplified in it and induce signal on the strips. The distance between the top GEM and the drift electrode is 5mm, the distance between GEMs in the triple-GEM cascade is 1.5 mm and the distance between the bottom GEM and the strips is 2.5 mm. The inner radius of the multi-strip structure is 350 mm, the strip length is 30 mm, the strip pitch is equal to 0.2 mm at the inner side and the number of strips is 2048. Thus the angular aperture of the first detector is about 67 degrees.

The OD4 will be equipped with custom made electronics that is designed to work in counting mode with one discriminator threshold. Each channel contains preamplifier, discriminator and scaler. If a photon produces the signal higher than the discriminator threshold, it is counted by the scaler and photon position is associated to a strip number.

The OD4 is designed to work with low energy photons with energy from 5 keV to 15 keV and is filled with Ar-CO_2 (75-25%) gas mixture at 1 atm.

The final electronics for full size detector are not yet ready, and for the testing of main parameters only 32 channels in the central part were equipped with electronics. The detector was installed at the SR line at the VEPP-3 storage ring. For all the measurements monochromatic beam of 8.3 keV photons was used.

2012 JINST 7 C03021

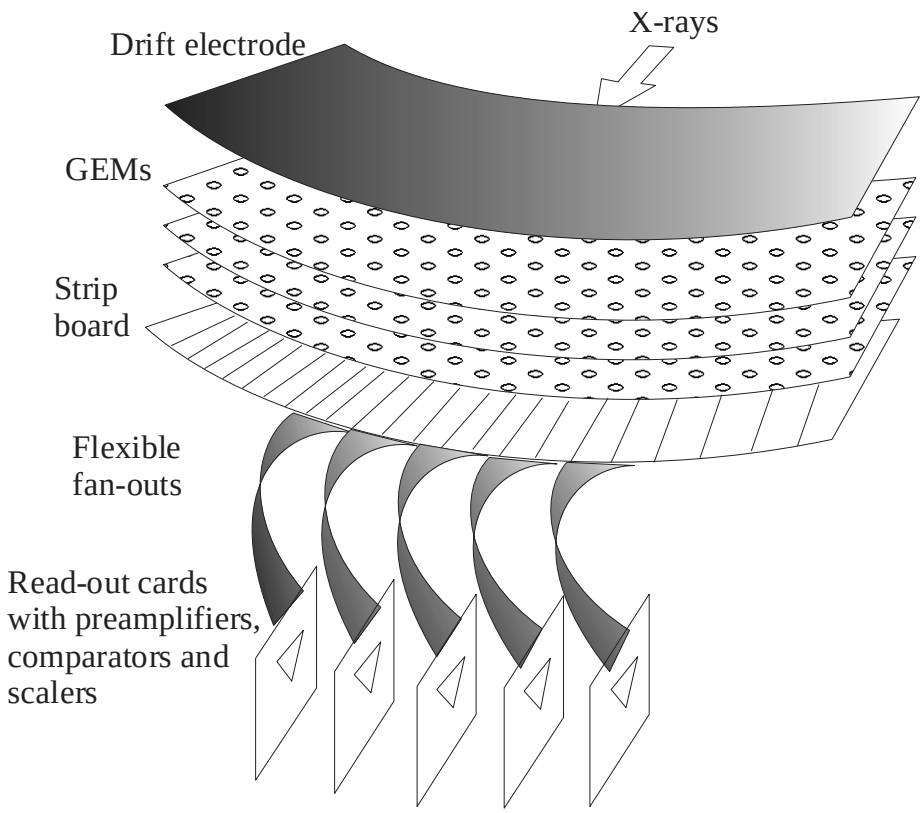

Figure 5. Schematic view of the OD4 design.

In figure 6 the relative counting rate as a function of the voltage on resistive divider and single GEM is presented for different discriminator thresholds. The relative counting rate was determined for each curve as a ratio of actual counting rate to the average rate on the plateau. The irradiation was performed with narrow 20 μm wide beam aligned at the center of one channel. At the points where the relative rate is equal to 0.5, the signal produced by a single photon is equal to the value of the discriminator threshold. Using the data from electronic calibration we can calculate the corresponding gain values that are shown in figure 7 together with the extrapolation curve for higher GEM voltages.

For characterization of spatial resolution of the OD4 the channel response curve was measured. The detector was scanned with 20 μm wide X-ray beam and counting rate of several channels was measured. During this measurement the high voltage at GEMs and the discriminator threshold were kept at the values that provided 90% detection efficiency. The channel response curves for three neighbouring channels are shown in figure 8. The channel aperture(FWHM of the channel response curve) is equal to about 0.5 mm. It is wider than the channel pitch (0.2 mm) due to photoelectrons range and transverse diffusion of electrons on their path to the strip plane. However the value of channel aperture of 0.5 mm is enough to achieve the main objective of the OD4: to distinguish the points at an angular distance of 0.1 degree.

One of the advantages of GEM-based detectors is their high rate capability. This parameter is important for application for WAXS because it determines the exposure time and thus affects time

2012 JINST 7 C03021

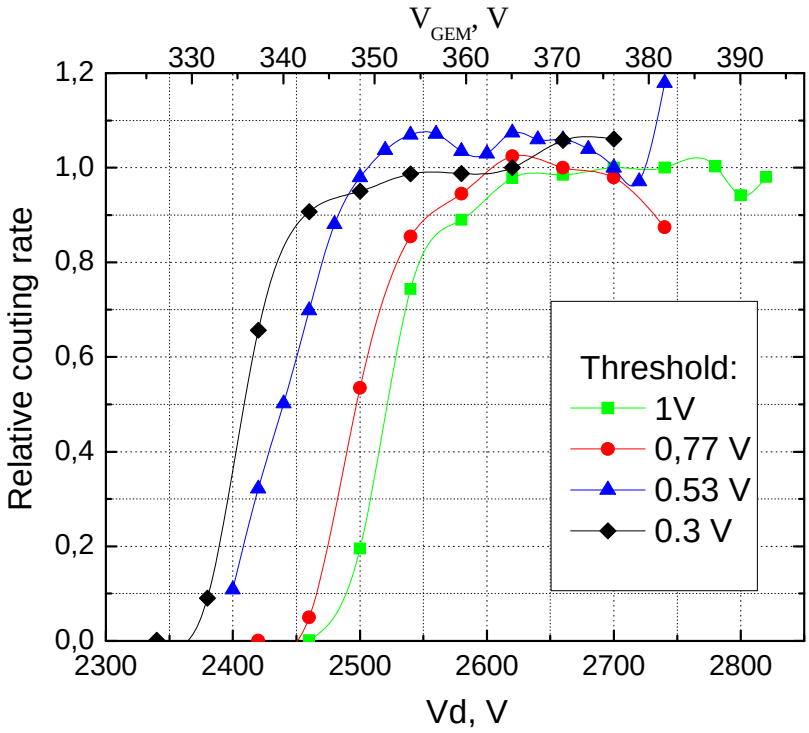

Figure 6. Counting rate of the OD4 detector channel as a function of voltage on the resistive divider and GEM for different values of the discriminator threshold.

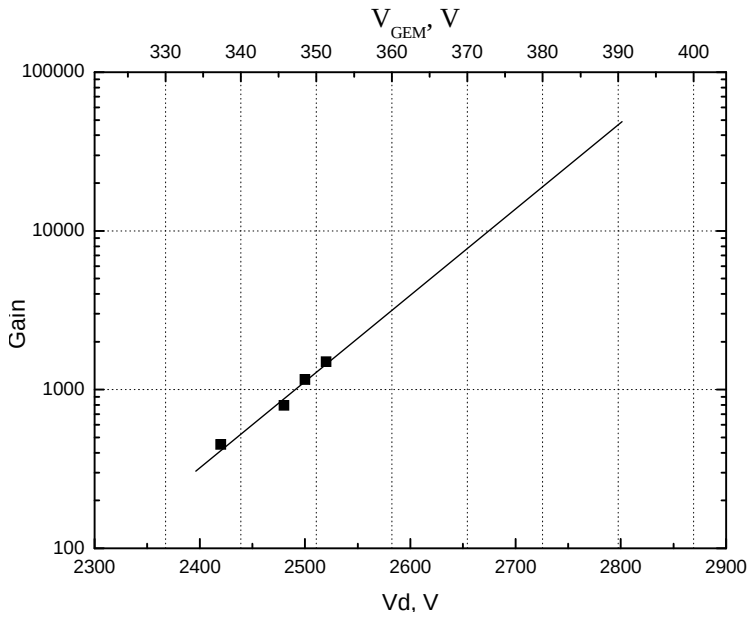

Figure 7. The OD4 detector gain as a function of voltage on the resistive divider and GEM.

resolution of the dynamic studies. The result of the measurement of OD4 rate capability is shown in figure 9. Details of the conditions of this measurement can be found in [11]. There is no degradation

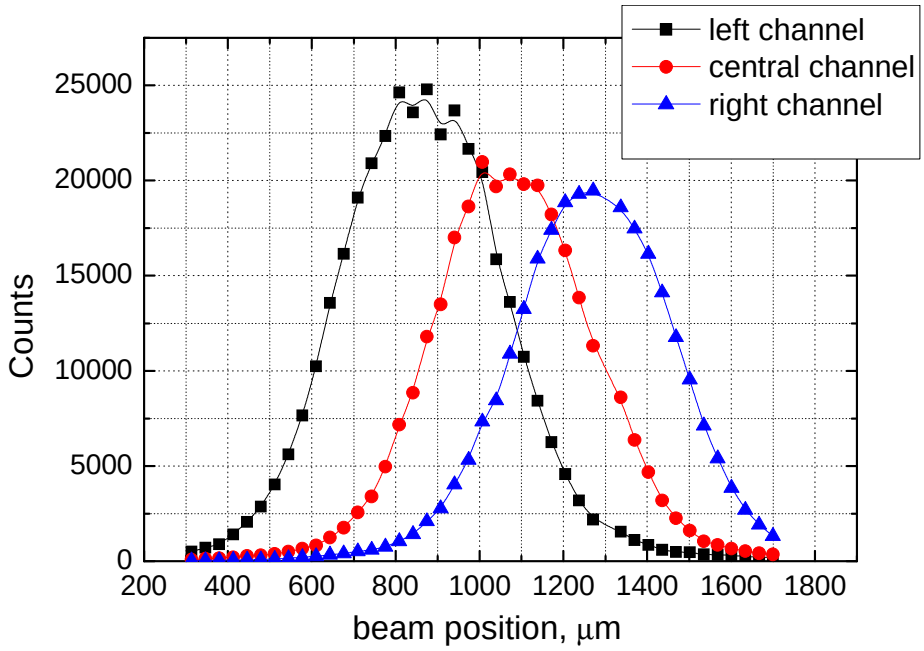

Figure 8. Channels response as a function of beam position.

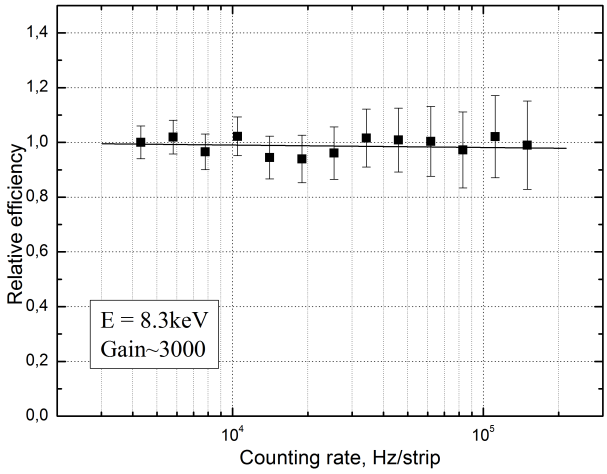

Figure 9. Rate capability of the OD4.

of efficiency observed till the maximum rate in the measurement of $\sim 2*10^5 counts/(channel*s)$.

The study of main parameters of the OD4 demonstrted that such detector is feasible. At present the full size detector fully equipped with electronics is under construction.

4 Triple-GEM detectors for the tagging system of the KEDR experiment

The KEDR detector on the VEPP-4M electron-positron collider [13–15] contains a unique tagging system (TS) that is intended for study of two-photon interactions [16, 17]. The TS uses the

2012 JINST 7 C03021

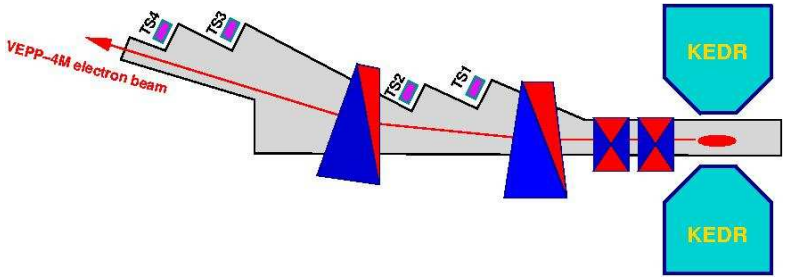

Figure 10. Schematic view of the KEDR tagging system.

accelerator magnets as part of the spectrometer as shown in figure 10. The dipole magnets allow registering electrons and positrons leaving the interaction point at zero angle after loosing part of their energy in photon-photon interaction. For simplicity such particles will be called as "scattered electrons" (SE) below. The lower energy SE is taken away from the equilibrium orbit with the help of vertical magnetic field and then detected in one of the four tagging system stations TS_1-TS_4. The quadrupoles focus SEs in such a way that their transverse coordinates in the detector planes almost do not depend on their initial angle. Thus measuring the coordinate one can unambiguously determine the particle energy.

Initially the tagging system included 8 stations based on drift tubes which allowed measuring the SE track coordinate in the beam orbit plane with an average resolution of $\sim$300 μm [16, 17]. For the purpose of improving the spatial resolution and adding the possibility of rejection of the single Bremsstrahlung (SBS) background,the upgrade of the system was performed [18–20]. Each TS station was supplemented with a high resolution two-coordinate detector based on cascaded GEM) in front of it.

Each detector for the TS upgrade contains a cascade of 3 GEMs with a spacing of 1.5 mm. Each GEM has a hexagonal structure of holes of 80 μm in diameter with a pitch of 140 μm. The GEM thickness is 50 μm. The distance between the bottom GEM and the readout printed circuit board(PCB) is 2mm and the distance between the top GEM and the drift electrode is 3mm.

The PCB contains 2 layers that are shown schematically in figure 11. The top layer(straight strips) contains strips 60 μm wide. The bottom layer(stereo strips) consists of strips 150 μm wide that are divided into straight sections and bridges connecting neighboring sections so that a stereo strip is on an average inclined at a certain angle relative to the straight strips. Such configuration of the bottom layer provides uniform charge induction that does not depend on the position along a strip.Straight sections of the stereo strips have different length depending on the position in the detector. In the central area, up to 1cm from the central plane of the detector the straight sections are 1mm long that provides the angle between stereo and straight strips to be equal to 30°. Outside this area the straight sections are 5 mm long and the angle between stereo and straight strips is close to 11°.Such layout provides better spatial resolution in the vertical direction in the central area which corresponds to the region around the orbit plane. The GEMs and PCBs were produced by the CERN workshop.

Two types of detectors were designed. Stations TS4 are equipped with detectors of a 256x100

2012 JINST 7 C03021

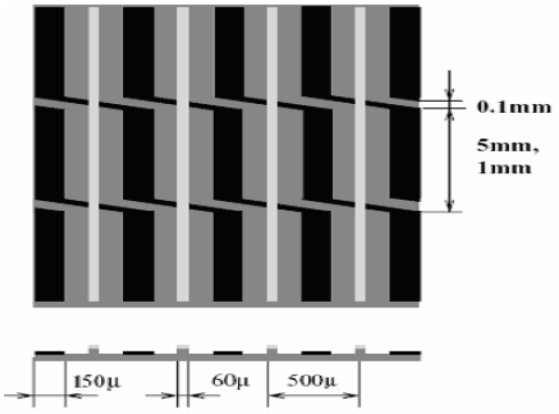

Figure 11. Schematic view of the PCB with small angle stereo readout. Straight strips marked as light grey, stereo strips marked as black. Straight sections of the stereo strips have different length, depending on the position in the detector. This is marked as 1 mm and 5 mm pointing at the straight section.

mm^2 sensitive area. Stations TS1-TS3 contain detectors with a 128x100 mm^2 sensitive area. Each large detector has 1024 channels (512 in the straight layer and 512 in the stereo one). Each small detector has 512 channels (256 in the straight layer and 256 in the stereo one). 4 spare detectors were also assembled (1 large and 3 small ones) and have been used for tests in the cosmic-ray set-up.

A study of main parameters of the GEM detectors was performed with a series of tests with cosmic particles. Detailed description of the set-up and results of these tests can be found in [19, 20]. Three detectors were fixed one over another at a distance of about 3 cm with plastic scintillation counters on the top and the bottom of the stack. The trigger signal was formed on coincidence of signals from the scintillation counters. The detectors operated with an Ar-25%CO_2 gas mixture. The efficiency was determined as the ratio of events with tracks that caused signals in both the straight and inclined strips of the central detector to all events with tracks that produced signals in the top and bottom detectors.The dependence of the efficiency on gas amplification in the detector is shown in figure 12. The gas gain here was determined via measuring the average sum of signals from the straight and the inclined strips and correcting it with the coefficient defined by electronic calibration.

From the figure we can see that the efficiency plateau starts at a gain of $\sim$25000 and the plateau level is around 98%. The measurements of spatial resolution were performed at a gain of $\sim$30000. The result of the measurement of spatial resolution in the direction perpendicular to the straight strips is shown in figure 13. The figure demonstrates the distribution of residuals, i.e. the difference between the calculated coordinate of the point where a track crosses the detector and the measured position of this track. The track position was determined from signals in the detector channels by the Center of Gravity (COG) method.

The fitted standard deviation of the distribution in the figure is 89 μm. Since the detectors were expected to be similar, the resolution can be calculated from this figure as $\sigma_{det} = \sigma_{meas}/\sqrt{3/2}$, where σ_{det} is the resolution of the detector and σ_{meas} is the measured standard deviation. The resolution of the detector is equal to $\sim$73 μm.

2012 JINST 7 C03021

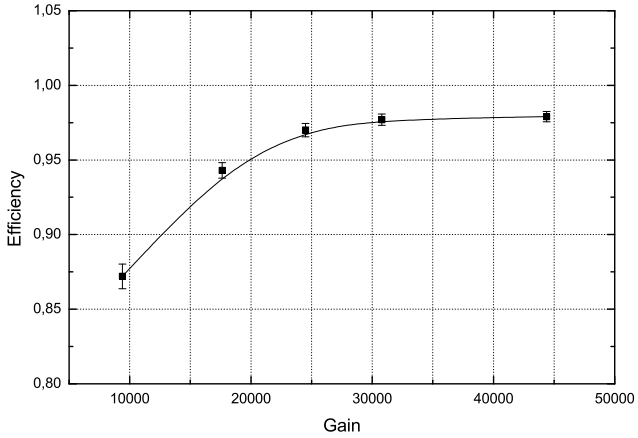

Figure 12. Efficiency of the TS triple-GEM detector as a function of gas gain measured with cosmic particles. The efficiency was determined as the ratio of events with tracks that caused signals in both the straight and inclined strips of the central detector to all events with tracks that produced signals in the top and bottom detectors.

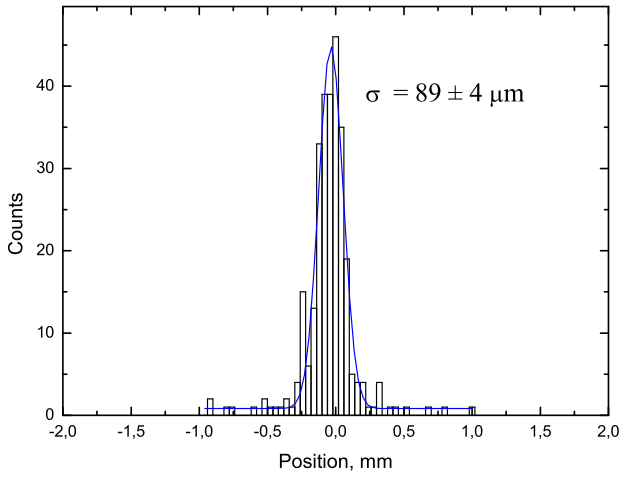

Figure 13. Distribution of residuals of the TS triple-GEM detector in the direction perpendicular to the straight strips. The derived intrinsic resolution of the detector is equal to $\sim$73 μm

Installation of all triple-GEM detectors in the TS was completed in the beginning of 2009. During the season of 2009-2010, operation of the GEM DAQ was refined and the system was being started. At the beginning of the season 2010-2011 (November 2010), the GEM system was included in the KEDR DAQ. Detailed description of the detector electronics and data acquisition system can be found in [20].

High quality tracks from the TS stations were selected for analisys of the operation of the GEM detectors together with drift tubes hodoscopes. Then the GEM detectors were scanned for charge clusters in both the straight and inclined layers in a certain position corridor around the reconstructed tracks. The GEM detector is considered efficient if charge clusters are found in both

2012 JINST 7 C03021

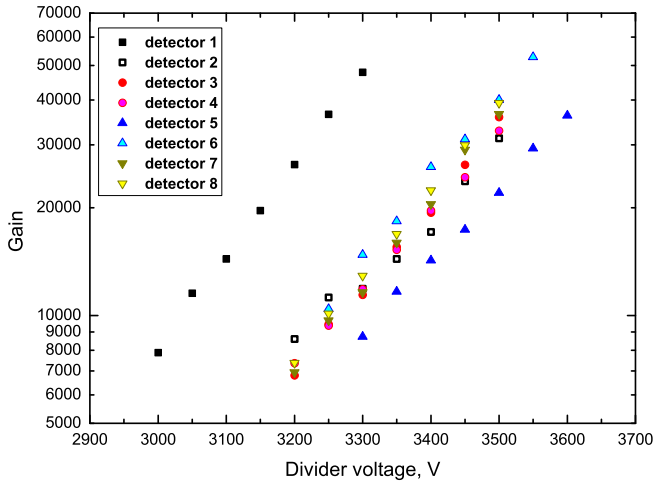

Figure 14. Gain as a function of voltage on the resistive divider for the 8 detectors of the TS-GEM system.

the straight and inclined layers.

The results on the main detectors parameters such as gas amplification and efficiency are shown in figures 14, 15. Figure 14 presents the dependence of the TS-GEM detector gain on the resistive divider voltage. The gain value is obtained from the sum of signals in both layers by multiplying the calibration constant obtained by electronic calibration. All the detectors demonstrate exponential gain-voltage characteristics. Detector 1 and detector 5 show a gain substantially different from that of the other 6 detectors due to deviations in the resistive divider parameters. The maximum gain of 40000-50000 is not limited by a discharge, but the measurement was stopped at these points because a substantial fraction of signals was limited by the dynamic range of the front-end amplifiers.

Figure 15 shows the dependence of the efficiency on the gain of the detectors for all the 8 GEM detectors. All the detectors except detector 2 and detector 5 show a very similar behavior with efficiency close to 90% at a gain value of 20000 and efficiency plateau level between 95% and 98%. This is rather close to the result of the measurement with cosmic particles (see figure 12). The GEM detectors work in a rather noisy environment very close to the beam. Detectors 1,2,5,6 are disposed 25 mm from the beam, and detectors 3, 4, 7 and 8 are 50 mm from the beam. The high level of pick-up noise often causes some excess pedestal fluctuations which are crucial for selection of charge clusters. The higher pedestal noise is the most probable reason for the smaller efficiency plateau in the case of detectors 2 and 5 in figure 15. Nevertheless, both the detectors have efficiency close to 93% at a gain of $\sim$30000.

Stability of the GEM detectors during the beginning of 2010-2011 run is demonstrated in figures 16, 17.During the first month of operation, the high voltage on the detectors was tuned for reaching a gain higher than 20000 in all the detectors, even when atmospheric pressure is getting to its highest values. As we can see in figure 16, the gain exhibits synchronous changes in all the detectors following the atmospheric pressure. After such tuning, the efficiency in all the detectors is kept higher than 95%.

2012 JINST 7 C03021

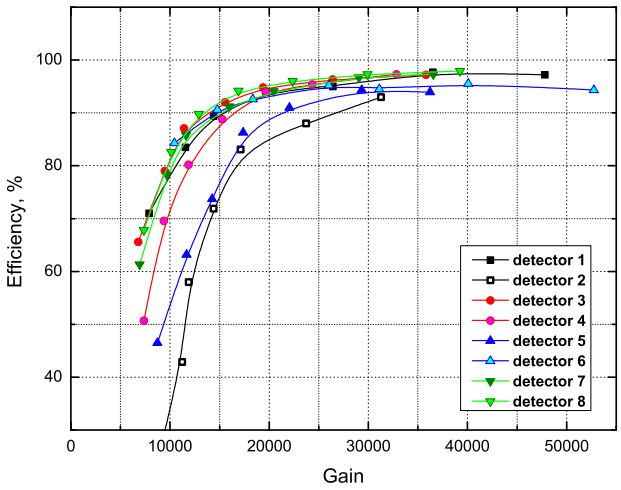

Figure 15. Efficiency as a function of gain for the 8 detectors of the TS-GEM system.

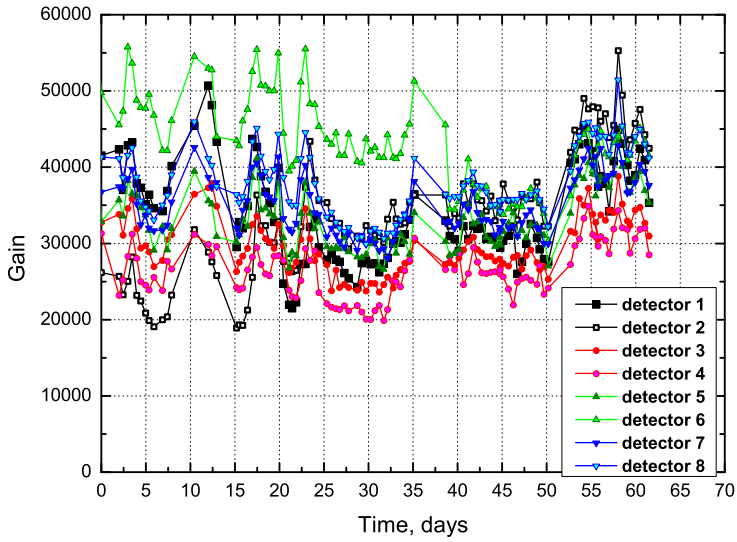

Figure 16. Gain as a function of time for the 8 GEM detectors during the first months of operation.

5 The tagging system of the Deuteron experiment

The method of an internal target in a charged particle storage ring was proposed and first used in nuclear-physics experiments in the late 1960s at the Institute of Nuclear Physics (INP), Siberian Branch of the Russian Academy of Sciences, Novosibirsk [24, 25]. The internal gas target of the storage ring [26] consists of polarized deuterium atoms injected in the form of a jet with an intensity of $8*10^{16}$ at s^{-1} into a thin-walled T-shaped storage cell with open edges. Bouncing from the cell walls, the atoms can multiply cross the electron beam circulating through it, thereby increasing the target thickness. Almost all advantages of the internal-target technique have been realized at INP over the succeeding period. For example, a number of experiments were conducted at the VEPP-2 electron storage ring to study the properties of light nuclei with coincidence detection of

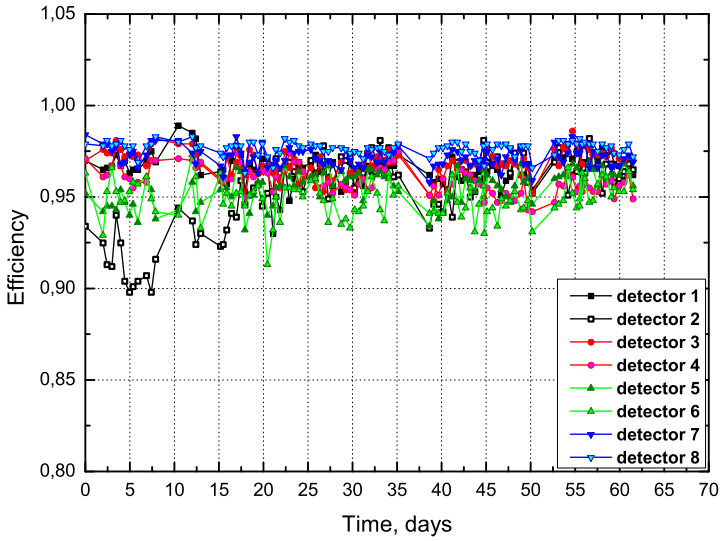

Figure 17. Efficiency as a function of time for the 8 GEM detectors during the first months of operation.

the scattered electron and nuclear decay products, including the slow particles. Experiments with a tensor-polarized deuterium gas target have also been conducted here for the first time.

Further progress of the experiments is associated with the introduction of an almost-real photon tagging system (PTS) at VEPP-3 ([25]). It will allow a series of measurements of the polarized observables with photon energies up to 1.5 GeV to be made in various reactions with photon absorption. For example, the deuteron photodisintegration experiment, where, according to unpolarized measurements, the transition to a quark-gluon description of the reaction is observed already at an energy $\sim$1 GeV [27], is expected to be continued.

PTS is located inside the experimental straight-line section and does not disrupt the storage ring beam optics (figure 18). PTS has three "warm" dipole magnets (D1,D2,D3) with magnetic field integrals of 0.248, 0.562, and 0.314Tm. The internal target (SC) lies between the first and second magnets. The electrons that lost their energy through a particular reaction on the target and that retained the direction of their motion close to the initial one are deflected from the storage ring beam trajectory by the strong field of the second magnet and are expelled through a window from the vacuum chamber of the storage ring. The system of position-sensitive detectors based on cascaded GEMs determines the flight coordinates of these electrons; a trigger sandwich scintillator is located after the position-sensitive detectors. Anticoincidences with the sandwich scintillator (S1,S2) allows most of the events from the bremsstrahlung of electrons on target nuclei to be rejected.

Three triple-GEM detectors are planned to be installed in the PTS. In general the detector design will be very similar to that of the detectors for the KEDR TS. The detector sensitive area will be 150*40 mm^2. The readout board will contain two layers: the inclined and the straight strips. The inclination angle will be 30 degrees. Multiple scattering in the detector material will affect the track position resolution in the PTS unlike the KEDR TS, where only one high resolution detector is installed just after the outlet window in each station. In order to minimize multiple scattering the detector elements will have reduced thickness of copper down to 1-2 μm at each GEM side. Such approach was investigated in [28] and it was found that the reduction of copper layers does

2012 JINST 7 C03021

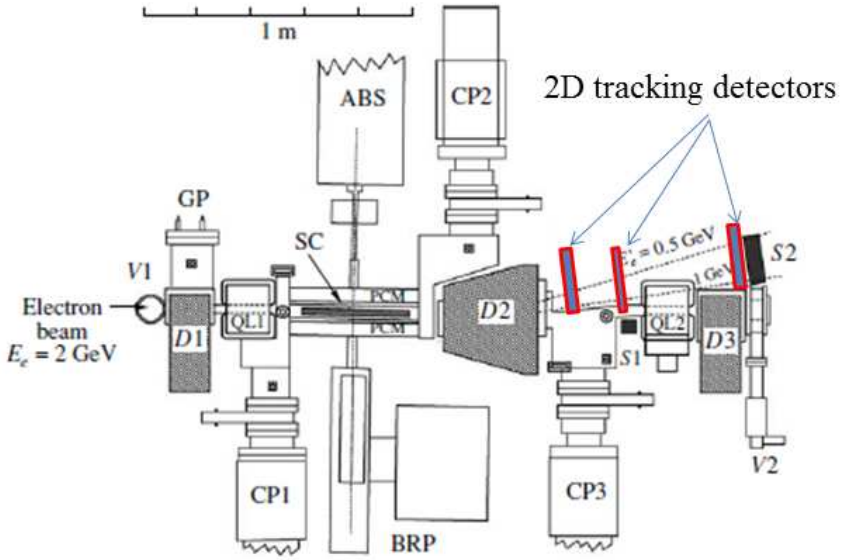

Figure 18. Schematic view of the almost-real photon tagging system (top view). D1, D2, D3 — three dipole magnets in the tagging system; QL1, QL2 quadrupole lenses; PCM — target polarization controlmagnet; S1, S2 — trigger sandwich scintillators; ABS — polarized atomic beam source; SC — target storage cell; BRP — Breit-Rabi polarimeter for ABS jet atoms; CP1, CP2, CP3, GP — cryogenic and getter pumps; V1, V2 — gate valves of the experimental section.

not affect the detector performance. Triple-GEM detector with reduced copper layers will have material budjet of $\sim 0.15\% X_0$ that will decrease the influence of multiple scattering on the spatial resolution of the detectors in the PTS below 100μm.

6 Conclusions

Micro-pattern gas technology is actively used at Budker INP. This review describes four projects where GEMs are applied in X-ray detectors and particle tracking detectors. In all cases the use of GEM is dictated by high particle rate and high spatial resolution needed in each application. Two projects are almost completed, these are: DIMEX — the detector for imaging of explosions at SR beam, and the triple-GEM detectors for the tagging system of the KEDR detector at the VEPP-4M collider. The final version of the DIMEX is currently used at the station ”VZRYV” at the VEPP-3 storage ring, and another station with the DIMEX is under construction at the SR line of the VEPP-4M storage ring. The tagging system of the KEDR detector successfully worked during the season 2010-2011 with all triple-GEM detectors in operation with the efficiency above 95%. The detector for WAXS studies (OD4) with arc-shaped cascaded GEM as the amplifier is under construction now. The final version of the electronic board that will include also the readout strip structure of the detector is being designed. The Photon tagging system (PTS) of the Deuteron experiment at the VEPP-3 storage ring is new project that was proposed last year. The system is planned for installation at the storage ring in two years from now.

2012 JINST 7 C03021

Acknowledgments

This work was partly funded by RFBR grants 08-02-01155, 09-02-01143-a, 10-02-00871-a, by the Ministry of Science and Education of the Russian Federation and by Grant of the Government of Russian Federation (11.G34.31.0047).

References

[1] F. Sauli, *GEM: A new concept for electron amplification in gas detectors*, *Nucl. Instrum. Meth.* **A 386** (1997) 531.

[2] V. Aulchenko, P. Papushev, S. Ponomarev, L. Shekhtman and V. Zhulanov, *Development of a one-dimensional detector for the study of explosions with a synchrotron radiation beam*, *J. Synchrotron Rad.* **10** (2003) 361.

[3] V. Aulchenko et al., *Development of fast one-dimensional X-ray detector for imaging of explosions*, *Nucl. Instrum. Meth.* **A 513** (2003) 388.

[4] V. Aulchenko et al., *Detector for imaging of explosions: Present status and future prospects with higher energy X-rays*, 2008 *JINST* **3** P05005.

[5] V.M. Aulchenko et.al., *Current status and further improvements of the detector for imaging of explosions*, *Nucl. Instrum. Meth.* **A 603** (2009) 73.

[6] R. Horisberger and D. Pitzl, *A Novel readout chip for silicon strip detectors with analog pipeline and digitally controlled analog signal processing*, *Nucl. Instrum. Meth.* **A 326** (1993) 92.

[7] S. Bachmann et al., *Charge amplification and transfer processes in the gas electron multiplier*, *Nucl. Instrum. Meth.* **A 438** (1999) 376.

[8] J. Beutel, H.L. Kundel and R.L. Van Metter (eds), *Handbook of Medical Imaging. Volume 1. Physics and Psychophysics*, SPIE Press (2000).

[9] V.M. Titov et al., *Experience of using synchrotron radiation for studying detonation processes*, *Combustion Explos. Shock Waves* **47** (2011) 615.

[10] V.M. Aulchenko et al., *A new one-coordinate gaseous detector for WAXS experiments (OD4)*, *Nucl. Instrum. Meth.* **A 575** (2007) 251.

[11] V. Aulchenko et al., *Development of one-coordinate gaseous detector for wide angle diffraction studies*, 2008 *JINST* **3** P04008.

[12] V.M. Aulchenko et.al., *Progress with one-coordinate detector for WAXS*, *Nucl. Instrum. Meth.* **A 603** (2009) 69.

[13] V. Anashin et al., *Status of the KEDR detector*, *Nucl. Instrum. Meth.* **A 478** (2002) 420.

[14] V. Anashin et al., *VEPP-4M Collider: Status and Plans*, in *Proc. of EPAC'98*, Stockholm Sweden (1998), p. 400.

[15] V. Smaluk for the VEPP-4 team, *Accelerator Physics Issues of the VEPP-4M at Low Energy*, in *Proc. of EPAC 2004*, Luzern Switzerland (2004), p. 749.

[16] V. Aulchenko et al., *Detector KEDR tagging system for two photon physics*, *Nucl. Instrum. Meth.* **A 355** (1995) 261.

[17] V. Aulchenko et al., *Detector KEDR tagging system for two photon physics*, *Nucl. Instrum. Meth.* **A 379** (1996) 360.

2012 JINST 7 C03021

[18] V. Aulchenko et al., *Upgrade of the KEDR tagging system*, *Nucl. Instrum. Meth.* **A 494** (2002) 241.

[19] V. Aulchenko et al., *Triple-GEM detectors for KEDR tagging system*, *Nucl. Instrum. Meth.* **A 598** (2009) 112.

[20] V. Aulchenko et al., *Operation of the triple-GEM detectors in the tagging system of the KEDR experiment on the VEPP-4M collider*, 2011 *JINST* **6** P07001.

[21] B. Ketzer et al., *Triple GEM tracking detectors for COMPASS*, *IEEE Trans. Nucl. Sci.* **49** (2002) 2403.

[22] A. Bressan, J. Labbe, P. Pagano, L. Ropelewski and F. Sauli, *Beam tests of the gas electron multiplier*, *Nucl. Instrum. Meth.* **A 425** (1999) 262.

[23] S. Bachmann et al., *Discharge mechanisms and their prevention in the gas electron multiplier (GEM)*, *Nucl. Instrum. Meth.* **A 479** (2002) 294.

[24] S. Popov, *Internal targets in storage rings for charged particles*, *Phys. Atom. Nucl.* **62** (1999) 256 [*Yad. Fiz.* **62** (1999) 291].

[25] D. Nikolenko et al., *Experiments with internal targets at the VEPP-3 electron storage ring*, *Phys. Atom. Nucl.* **73** (2010) 1322. [*Yad. Fiz.* **73** (2010) 1365].

[26] M. Dyug et al., *Internal polarized deuterium target with cryogenic atomic beam source*, *Nucl. Instrum. Meth.* **A 495** (2002) 8.

[27] CLAS collaboration, P. Rossi et al., *Onset of asymptotic scaling in deuteron photodisintegration*, *Phys. Rev. Lett.* **94** (2005) 012301.

[28] A. Bondar et al., *Light multi-GEM detector for high-resolution tracking systems*, *Nucl. Instrum. Meth.* **A 556** (2006) 495.

2012 JINST 7 C03021